

# Ring Laser Measurements of Ground Rotations for Seismology

K. U. Schreiber<sup>2</sup>, J. N. Hautmann<sup>1</sup>, A. Velikoseltsev<sup>2</sup>, J.  
Wassermann<sup>1</sup>, H. Igel<sup>1</sup>, J. Otero<sup>3</sup>, F. Vernon<sup>3</sup>, and J.-P. R. Wells<sup>4</sup>

<sup>1</sup> *Department of Earth and Environmental Sciences,  
Ludwig-Maximilians-University Munich  
Theresienstrasse 41, D-80333 Munich, Germany*

<sup>2</sup> *Technische Universitaet Muenchen,  
Forschungseinrichtung Satellitengeodaesie  
Fundamentalstation Wettzell, 93444 Bad Kötzing, Germany \**

<sup>3</sup>*Cecil H. and Ida M. Green Institute of Geophysics and Planetary Physics,  
Scripps Institution of Oceanography University of California,  
San Diego 9500 Gilman Drive,  
La Jolla, CA 92093-0225, USA*

*and*

<sup>4</sup> *Department of Physics and Astronomy,  
University of Canterbury, Private Bag 4800,  
Christchurch 8020, New Zealand.*

(Dated: July 5, 2008)

## Abstract

Since the discovery of the wave nature of light, optical interferometry has assumed an important place in high precision metrology. This is mostly due to the inherent high sensor resolution for operational wavelengths in the vicinity of several hundred nanometers. In this context, interferometers in the Michelson configuration are most prominently used in gravitational wave antennas, such as the large projects VIRGO, LIGO and GEO600. In the Sagnac configuration they are used for high resolution rotation monitoring such as the precise observation of Earth rotation. Modern large scale ring lasers reach a sensitivity for the measurement of rotation of 1 pico-rad/sec (with approx. 1 hour of averaging). Because of the comparatively short wavelengths employed, optical interferometers are extremely sensitive to small mechanical perturbations of the entire apparatus. These can be caused by deformations, thermal or mechanical stress and instabilities in the alignment of the optical components at the level of about  $\lambda/100$ . Ring lasers suitable for geophysical applications require a sensor resolution in the range of  $10^{-8}$  rad/s and below. This demands a scale factor of the instrument which is only achievable with mechanical dimensions of the interferometer of the order of about 1 m<sup>2</sup>. At the same time the necessary mechanical rigidity of the entire instrument has to be of the order of 5 nm. Currently this has only been achieved with monolithic ring lasers made from blocks of Zerodur and installed in a temperature stabilized underground environment. However if long term sensor stability is not required, compromises can be made and, in particular for studies of regional seismic events, it becomes feasible to build a heterolithic rotation sensor in a simpler and much cheaper way. Here we report the design and first results from the GEOSensor, which has been specifically constructed for studies in rotational seismology. The sensor is operated at the Piñon Flat Seismic Observatory in Southern California.

PACS numbers: 07.60.Ly, 42.60.By, 42.60.Da, 91.30.Px, 91.30.Ab

---

\*Electronic address: [schreiber@fs.wettzell.de](mailto:schreiber@fs.wettzell.de)

## 1. INTRODUCTION

Currently there are two types of measurements that are routinely used to monitor global and regional seismic wave fields. Standard inertial seismometers measure three components of translational ground displacement (velocity, acceleration) and form the basis for monitoring seismic activity and ground motion. The second type aims at measuring the deformation of the Earth (strains). It has been noted for decades (Aki & Richards (1980, 2002)) that there is a third type of measurement that is needed in seismology and geodesy in order to fully describe the motion at a given point, namely the measurement of ground rotation. The three components of seismically induced rotation have been extremely difficult to measure, primarily because previous devices did not provide the required sensitivity to observe rotations in a wide frequency band and distance range (the two horizontal components, equal to tilt at the free surface, are generally recorded at low frequencies, but are polluted by additional inertial effects). Indeed, Aki & Richards (2002) page 608 note that "seismology still awaits a suitable instrument for making such measurements". Furthermore, the motion amplitudes were expected to be small even in the vicinity of faults (Bouchon and Aki (1982)) whereas there is growing evidence that these amplitudes have been underestimated (e.g., Castellani and Zembaty (1996)). Following the pioneering observations with ring laser rotation sensors in Christchurch, New Zealand (McLeod et al. (1998); Pancha et al. (2000)) a purpose-built ring laser for the observations of the Earth's rotation rate located at Wettzell, Germany (Schreiber et al. (2006b)) was adapted to the sampling rate requirements in seismology allowing observations of earthquake-induced rotational ground motions over a wide magnitude and epicentral distance range (Igel et al. (2005, 2007); Schreiber et al. (2006a)). Analysis of these observations in combination with collocated recordings by a standard broadband seismometer showed the possibility of extracting additional seismograms on subsurface structure compared to translational measurements alone (e.g., Ferreira and Igel (2008); Fichtner and Igel (2008); Suryanto et al. (2007)), otherwise accessible with seismic array measurements only. These studies and earlier considerations motivated the development of a ring laser (denoted as the GEOsensor), specifically designed for seismological purposes given an observatory infrastructure. The prototype of this rotational sensor was installed at the Piñon Flat Observatory in 2005. The aim of this paper is to describe the technical details of this rotation sensor, to discuss issues related to the installation and

operation, and to show examples of earthquake induced rotation measurements from the GEOsensor. The comparison with collocated translational measurements confirm the previously established consistency with plane-wave theory and thus the validity of the rotation measurements (Igel et al. (2005)).

## 2. SENSOR DESIGN AND PROPERTIES

The high sensitivity for rotations of large ring lasers along with their insusceptibility to linear translations makes the application of these instruments very attractive for studies of rotational signals from seismic events. The required range of angular velocities to be measured is expected to be  $10^{-14}$  rad/s  $\leq \Omega_s \leq 1$  rad/s and the required frequency bandwidth for the seismic waves is in the range of  $3$  mHz  $\leq f_s \leq 10$  Hz (Schreiber et al. (2004b)). Three such devices mounted in orthogonal orientations will eventually provide the quantitative detection of rotations from shear, Love and Rayleigh waves, thus providing the missing quantities for a complete 6 degrees of freedom measurement system. Ring lasers are active interferometers, where two laser beams are circulating around a polygonal closed cavity in opposite directions (Aronowitz (1971)). If the whole apparatus is rotating with respect to inertial space one obtains a frequency splitting of the two counter propagating waves, which is proportional to the rate of rotation. The observed beat frequency  $\delta f$  is

$$\delta f = \frac{4A}{\lambda P} \vec{n} \cdot \vec{\Omega}, \quad (1)$$

where  $A$  is the area,  $P$  the perimeter enclosed by the beam path and  $\lambda$  the optical wavelength of the laser oscillation.  $\vec{\Omega}$  is the angular velocity at which the instrument is turning and  $\vec{n}$  is the normal vector to the laser beam plane. The resolution of a ring laser gyroscope increases as the size of the cavity increases. When first installed the GEOsensor reached a sensor resolution of  $\delta\varphi = 10^{-10}$  rad/s/ $\sqrt{s}$ . This outstanding sensitivity is suitable for the detection of both teleseismic waves and near source seismic signals. Typical seismic signals require high sensor stability for up to one hour of continuous data acquisition. This requirement is significantly reduced from the long-term stability necessary of an instrument for the measurement of Earth rotation variations (Schreiber et al. (2004a)), where the sensor drift has to be negligible over a timespan of many months. A ring laser for seismology must be capable of accurately recording seismic rotation rates while keeping the scaling factor (the

quotient in eq. 1) constant. At the same time the whole sensor must be relocatable, cost effective and allow for a relatively simple installation. Given the fact that a ring laser is a highly sensitive optical interferometer, all these requirements are essentially contradicting design goals. In order to achieve a workable concept, the interferometer is assembled from several individual components, (4 mechanically stable corner boxes with individually integrated alignment elements,) placed on a thick concrete platform, which provides the necessary rigid geometrical reference. In order to obtain a stable interferogram of the two laser beams the cavity length has to be kept constant to within a small fraction of a wavelength. Therefore ring lasers have to be placed in a temperature controlled underground laboratory (see discussion in subsection 3 B). The frequency band of interest for a rotational sensor in seismology covers about 5 orders of magnitude, while the corresponding sensitivity for the measurement of rotations should cover 14 orders of magnitude, the range between strong motions during a local earthquake on one side and the signals of an earthquake more than 10000 km away on the other side. However, if we exclude the strong motion domain from the immediate measurement of interest, we obtain a viable measurement range for a prototype sensor of approximately  $10^{-12} \text{ rad/s} \leq \Omega_s \leq 10^{-4} \text{ rad/s}$ , which still extends over 8 orders of magnitude. Most of this range is covered by large ring laser gyroscopes, such as the GEOSensor. Figure 1 gives an impression of the actually realized ring laser hardware. The laser cavity has the shape of a square. The 4 turning mirrors are each located inside adjustable stainless steel containers inside solid corner boxes. As shown in the right side of the plot, a folded lever system allows the alignment of each mirror mount to be within  $\pm 10$  seconds of arc. This high level of alignment is required to ensure lasing from an optically stable cavity. The steel containers in turn are connected together with stainless steel tubes, forming an evacuated enclosure for the laser beams. In the middle of one side the connecting steel tube is reduced to a small glass capillary of 4 mm in diameter and a length of 10 cm, which is required for gain medium excitation. When operated, the ring laser cavity is first evacuated and then filled with a mixture of helium and neon reaching a total gas pressure of approximately 6 hPa. The following two important considerations are unique for the GEOSensor design.

- Since the ring laser is constructed from several components, it requires a stable concrete platform base at the location of deployment. Such a pad is simple to specify and can be prepared totally independently of the actual GEOSensor deployment.

- The actual area of the ring laser component is not fully determined by the design. The instrument can be built according to the available space at the host observatory. Different GEOSensor realizations may therefore have different sizes and consequently different instrumental resolution. The length of the current instrument is 1.6 m on a side, which provides a total area of 2.56 m<sup>2</sup>.

In order to operate the GEOSensor, the cavity must be evacuated, baked and filled with a helium/neon gas mixture. This procedure requires a turbo molecular pump system and a manifold with a supply of <sup>4</sup>He, <sup>20</sup>Ne and <sup>22</sup>Ne. The pump system is not required during the operation of the GEOSensor but is necessary for the preparation of the sensor operation and used three to four times during a year in order to renew the laser gas. Laser excitation itself is achieved via a high frequency generator Stedman (1997), matched to a symmetrical high impedance antenna at the gain tube. A feedback loop maintains the level of intensity inside the ring laser and ensures monomode operation. When the ring laser is operated it detects the beat note caused by Earth rotation. The required high mechanical stiffness for the interferometer at the Piñon Flat Seismological Observatory is obtained from a 30 cm thick concrete slab, which makes up most of the laboratory floor. Figure 2 shows the realization of the rotation sensor. In the event of an earthquake the entire slab rotates rigidly without deformation and the Sagnac interferometer determines the rotation rate of the slab. The sensitivity of the ring laser is determined by the scale factor ( $4A/\lambda P$ ) of the instrument. In this expression  $A$  is the area circumscribed by the laser beams,  $P$  the effective length of the cavity i.e. the perimeter of the ring laser contour and  $\lambda$  the optical wavelength. Technically, the GEOSensor represents a continuous wave He-Ne laser system with a high quality factor of  $Q = \omega\tau = 474 \text{ THz} \times 0.001\text{s} \approx 10^{12}$ , with  $\tau$  being the ring down time of the laser cavity and  $\omega$  the frequency of the laser beam. The high Q value (together with the cavity dimensions) determines the extraordinary sensor resolution. Since the ring laser is rigidly tied to the ground at the Piñon Flat observatory the output signal is rate biased by Earth rotation, which generates the beat note (or “Sagnac” frequency). This rate bias offsets the earthquake signals from zero, i.e. away from the highly non linear lock-in region Wilkinson (1987). As discussed above,  $\vec{n}$  is the normal vector on the ring laser beam plane and  $\vec{\Omega}$  points along the rotational axis having a magnitude given by  $2\pi/86164 \text{ s}$  (1 revolution per sidereal day). At a latitude of 33.5 degrees north, corresponding to the location of the Piñon Flat Seismological Observatory in Southern California  $\delta f$  becomes

107.2 Hz for a horizontally oriented instrument. Seismically induced rotation signals show up as a frequency modulation of this otherwise constant Sagnac frequency caused by Earth rotation (Schreiber et al. (2005)). In practice the concrete slab of the ring laser installation is obviously slightly tilted towards south, so that the actually observed Sagnac frequency is around 102 Hz.

### 3. SENSOR PERFORMANCE AND OPERATIONAL ISSUES

#### A. Sensor Performance

When the ring laser cavity is filled with a mixture of helium and neon with a mixing ratio of 30:1, a radio frequency (RF) generator provides the necessary discharge to generate the laser beams to operate the gyroscope. Once the interferogram of the two counter-propagating laser beams is established one can determine the frequency of this beat note at a rate of 20 Hz. Using eq. 1 this translates into the instantaneous rate of rotation as is shown in fig. 3. With an integration time of 50 ms and the current performance of the frequency estimator the sensor resolution is as high as 20 nrad/s under stable operating conditions. This is enough to establish the rotation rate caused by teleseismic signals as well as a local seismic event. Figure 4 shows an example for a small local tremor generating rotation rates of approximately 150 nrad/s at maximum. Further examples of teleseismic earthquakes are presented and discussed in section 4. While the obtained sensor resolution is within one order of magnitude of the theoretical limit caused by shot noise (Schreiber et al. (2008)), there is still some room for improvement. In order to extract the variations of the Sagnac frequency from the Earth induced rate bias, a demodulation technique is employed. A voltage controlled oscillator (VCO) is slaved to the output frequency of the interferometer via a phase-locked loop (PLL). While the feedback voltage of the PLL serves as a voltage proportional to the rate of change of frequency, the sensor is still limited in resolution by how tightly the VCO can be locked to the input Sagnac frequency. A tight lock corresponds to a small capture range, which limits the dynamic range of the entire sensor. A sloppy lock on the other hand gives a wide dynamic range, but restricts the lower limit of the sensor's sensitivity. The current setup is a compromise, which excludes a very wide dynamic range and also reduces the available sensor sensitivity. However, there is a capacity to tune the

instrument as appropriate for either of the two limits of operation.

## B. Operational Issues

The GEOSensor is located in an underground laboratory in order to keep temperature fluctuations to a minimum. Despite all precautions the interferometer experiences temperature changes of several degrees even within one day. In response to that both the concrete foundation as well as the laser cavity expand or shrink by several  $\lambda$ , giving rise to perturbations of the interferogram because of longitudinal mode index changes. The effect of such “modehops” is shown in fig. 5. This complication was known in the design phase of the GEOSensor, but it was accepted because otherwise the construction would have become prohibitively expensive. Since local earthquakes are usually very short, this effect still allows the unambiguous reconstruction of the rotational ground motion during post-processing as fig. 5 demonstrates. While mode jumps in the case of large temperature gradients are frequent, they reduce to about one event per hour under normal operational conditions. Also visible is a slow drift in the observed Earth rotation rate, which is caused by dispersion effects in the laser gain medium. For teleseismic events a substantial reduction in the frequency of the mode jumps is desirable, because signals from remote earthquakes contain ground motion at much lower frequencies. Another complication is the possibility that a mode change results in a situation where two modes with different longitudinal index co-exist in the ring laser cavity. This causes the Sagnac frequency at 102 Hz to disappear. The rotational signal would still be there, but it is shifted in frequency by 46.875 MHz and therefore becomes inaccessible by the current detection electronics. An active perimeter control eventually will take care of these issues.

## 4. OBSERVATIONS

In 2006 and 2007 several earthquakes were recorded by the GEOSensor, located at the Piñon Flat Observatory, US. In this study, the rotational and translational signals measured by the ring laser component of the GEOSensor and the collocated seismometer, a Lennartz LE-3D 20s, are compared. Four events with diverse magnitudes and epicentral distances - and therefore varying frequency contents - are chosen to show the quality of the recorded

data. All information on the data is given in Table I. To evaluate the observed data and its consistency with theory (e.g., Igel et al. (2005)), the vertical component of rotation rate  $\vec{\Omega}_z$  is directly compared with the corresponding transverse acceleration  $\vec{a}$  according to:

$$\vec{\Omega}_z(x, t) = -\frac{\vec{a}(x, t)}{2c_p} \quad (2)$$

with  $c_p$  being the horizontal phase velocity underneath the measurement point. Assuming plane wave propagation and transverse polarization, the rotational and translational signals should match in waveform and the amplitude difference is two times the phase velocity. In order to analyse the recorded data, each of the events is lowpass filtered and processed depending on the individual frequency content. The transverse acceleration is obtained by the differentiation of the transverse component of translation in time, with respect to the backazimuth angle. The extent to which the phase between the signal obtained by the rotation sensor and the transverse acceleration agrees is quantified by the cross-correlation coefficient. This time dependent similarity is expressed by zero-lag cross-correlation coefficients with values between 0 and 1 (marking none or perfect agreement) as a function of time in a sliding time window. In Figure 7 the superposition of rotation rate and transverse acceleration for the M 7.6 Kamchatka event April 20, 2006 is presented. The time window with a length of 1200s presents the obtained rotation rate (dashed) and transverse acceleration (black) as a function of time (middle). Two enlarged plots (top) emphasize the similarity in waveform of the signals in two selected time windows. In the bottom plot the cross-correlation coefficient is presented as a function of time. Clearly visible is the strong increase in correlation with the surface wave arrival to a maximum coefficient of 0.95. Noticeable is the high level of cross-correlation in the surface wave section, around 0.8 before going back to 0.5 and below. According to eq. 2, the estimated peak phase velocity results to  $c_p = 5197m/s$ . The rotational seismogram of a regional earthquake, the M 5.4 Mexico event May 24, 2006 is shown in fig. 8, again compared to transverse acceleration. The sections of highest cross-correlation coefficients are enlarged (top plots). Before the Love wave onset, a cross-correlation coefficient less than 0.5 can be determined, which increases to a high value during the entire event with a maximum coefficient of 0.92. The corresponding peak phase velocity accounts to  $c_p = 4648m/s$ . To demonstrate the GEOsensor's ability for obtaining the rotation rate from local events, two California earthquakes presented in fig. 9 and fig. 10 were chosen. Both events are shallow, 4 km and 12 km (respectively) and have a

epicentral distance of less than  $1^\circ$ . Figure 9 shows the M 3.6 event May 20, 2007 and fig. 10 the M 3.9 event May 24, 2007. A clearly visible good fit in phase between rotation rate and transverse acceleration during the s-wave section is supported by a peak in cross-correlation coefficients for both superposition plots. The largest cross-correlation values reach 0.96 and 0.98 respectively. The apparent mismatch in waveform following the s-wave section can be explained by a reduced validity of the plain wave assumption for events with very low epicentral distances. The resulting maximum phase velocities are relatively high with values of  $c_p = 8670m/s$  and  $c_p = 14512m/s$ . These high phase-velocities are likely to be caused by the oblique incidence of the body wave phases as observed in Igel et al. (2005). The overall good fit in waveform demonstrates the suitability of the GEOsensor for geoscientific studies over a wide range of distances and magnitudes. The presented cross-correlation coefficients affirm expectations from theory, even though fig. 9 and fig. 10 are detained by the invalid plane wave assumption for small distances.

## 5. DISCUSSION AND CONCLUSIONS

Despite decades of high-quality broadband seismometry there are still issues that are poorly understood. This relates in particular to the components of rotations around three orthogonal axes to which - at least in general - translational sensors are also sensitive to and thus contaminated by. The two components of rotation around the horizontal axes are usually referred to as tilts (at the free surface). Tiltmeters are sensitive to horizontal accelerations and are thus not capable of providing a pure rotational signal. The advent of ring laser technology (originally designed for geodetic purposes) has led to the first accurate recordings of co-seismic rotations primarily around the vertical axis (e.g. Igel et al. (2005); Pancha et al. (2000)). These observations motivated the development of the GEOsensor, a ring laser sensor specifically designed for seismology, as reported here. Due to the short wavelength used in a laser-based optical instrument they are very sensitive to environmental effects such as temperature and pressure changes. The effects on the rotational measurements (e.g. longitudinal mode changes) have been illustrated above, in large parts due to the large temperature fluctuations at the Piñon Flat Observatory. Nevertheless a large set of data has been accumulated, demonstrating the consistent observation of rotational ground motions, when compared to recordings of standard seismometers. This has been previously

shown for the much more expensive monolithic ring laser system in Wettzell, Germany. While efforts are underway to understand the performance of alternative rotation sensors (Wassermann et al. (2008)) with much smaller dynamic range, which might be applicable in the near field under certain limited circumstances, there still is a need to investigate the fundamental physics of observing **complete** ground motion. This has relevance for large scale experiments like the gravitational wave detection (e.g. VIRGO and LIGO) where the quality of the observations strongly depends on decoupling the observing system from the ground motions in the 1 Hz regime. This is only possible if all components are known. In the light of this we propose to establish multi-component seismic observatories (displacements, velocities or accelerations and rotations, plus strain) combined with (i.e. surrounded by) a small-aperture broadband array, with which cross-validation (e.g. Suryanto et al. (2007); Wassermann et al. (2008)) is possible.

## 6. ACKNOWLEDGEMENTS

This work was supported by the Bundesministerium für Bildung und Forschung (BMBF), Grant 03F0325 A-D under the Geotechnology Program and DFG Grant Ig16/8. HI acknowledges support through a Cecil-and-Ida Green Fellowship of the SCRIPPS Institution of Oceanography, La Jolla.

- 
- Aki, K. and P.G. Richards, *Quantitative seismology*, 1st Edition, Freeman and Company (1980)
- Aki, K. and P.G. Richards, *Quantitative seismology*, 2nd Edition, University Science Books (2002)
- F. Aronowitz, (1971) The laser gyro. Laser applications, Vol. 1, edited by M. Ross, 133–200, Academic Press, New York
- Aronowitz, F. (1999), Optical Gyros and their Application, RTO AGARDograph 339 *Fundamentals of the Ring Laser Gyro*, (1999)
- Bouchon, M.B., K. Aki; *Strain, tilt, and rotation associated with strong ground motion in the vicinity of earthquake faults*. Bull. Seism. Soc. Amer., 1717:1738 – 72 (1982)
- Castellani, A., Z. Zembaty; *Comparison between earthquake spectra obtained by different experimental sources*. Engng Struct., 597:603 – 18 (1996)

- Cochard, A., H. Igel, B. Schuberth, W. Suryanto, A. Velikoseltsev, K.U. Schreiber, J. Wassermann, F. Scherbaum, D. Vollmer *Rotational Motions in Seismology: Theory, Observation, Simulation*. Springer Monograph: “Earthquake Source Asymmetry, Structural Media and Rotational Effects”, Chapter 30, (2006)
- Ferreira, A., H. Igel; *Rotational motions of seismic surface waves in a laterally heterogeneous Earth.*, (2008)
- Fichtner, A., H. Igel; *Sensitivity densities for rotational ground motion measurements*, Bull Seism. Soc. Amer., submitted., (2008)
- Igel, H., K.U. Schreiber, B. Schuberth, A. Flaws, A. Velikoseltsev, A. Cochard, *Observation and modelling of rotational motions induced by distant large earthquakes: the M8.1 Tokachi-oki earthquake September 25, 2003*. Geophys. Res. Lett, **32**, L08309, doi:10.1029/2004GL022336, (2005)
- Igel, H., A. Cochard, J. Wassermann, A. Flaws, K.U. Schreiber, A. Velikoseltsev, N. Pham Dinh; *Broad-band observations of earthquake-induced rotational ground motions*. Geophys. J. Int., 168:182 – 196, (2007)
- McLeod, D.P., G.E. Stedman, T.H. Webb, K.U. Schreiber, *Comparison of standard and ring laser rotational seismograms*. Bull. Seism. Soc. Amer., 88:1495 – 1503, (1998)
- McLeod, D.P., B.T. King, G.E. Stedman, K.U. Schreiber and T.H. Webb, *Autoregressive analysis for the detection of earthquakes with a ring laser gyroscope*. Fluctuations and Noise Letters, Vol. 1, No. 1:R41 – R50, (2001)
- Pancha, A., T.H. Webb, G. E. Stedman, D.P. McLeod and K.U. Schreiber, *Ring laser detection of rotations from teleseismic waves*. Geophys. Res. Lett., 27:3553 – 3556, (2000)
- Pritsch, B., K.U. Schreiber, A. Velikoseltsev, J.-P. R. Wells; *Scale Factor Corrections in Large Ring Lasers*.; Applied Physics Letters 91, 061115, doi:10.1063/1.2768639 (2007)
- Schreiber, K.U., M. Schneider, C.H. Rowe, G.E. Stedman and W. Schlüter, *Aspects of Ring Lasers as Local Earth Rotation Sensors*. Surveys in Geophysics, Vol. 22, Nos. 5-6:603 – 611, (2001)
- Schreiber, K.U., G.E. Stedman and T. Klügel ; *Earth tide and tilt detection by a ring laser gyroscope*. J. Geophys. Res. **108** (B)2, 10.1029/2001JB000569, (2003)
- Schreiber, K.U., A. Velikoseltsev, M. Rothacher, T. Klügel, G.E. Stedman, D.L. Wiltshire; *Direct measurement of diurnal polar motion by ring laser gyroscopes*. J. Geophys. Res. Vol. 109 No. B6, 10.1029/2003JB002803, B06405, (2004)
- U. Schreiber, A. Velikoseltsev, G.E. Stedman R.B. Hurst, T. Klügel, (2004) Large Ring Laser Gyros

- as High Resolution Sensors for Applications in Geoscience. Proceedings of the 11th International Conference on Integrated Navigation Systems, St. Petersburg, 326–331
- Schreiber, K.U., H. Igel, A. Velikoseltsev, A. Flaws, B. Schuberth, W. Drewitz, F. Müller; *The GEOsensor Project: Rotations - a New Observable for Seismology*. Springer Monograph: “Observation of the Earth System from Space”, 427 – 447, (2005)
- Schreiber, K.U., G.E. Stedman, H. Igel, A. Flaws; *Rotational Motions in Seismology: Theory, Observation, Simulation*. Springer Monograph: “Earthquake Source Asymmetry, Structural Media and Rotational Effects”, Chapter 29, (2006)
- Schreiber, K.U., G.E. Stedman, H. Igel, A. Flaws; *Ring laser gyroscopes as rotation sensors for seismic wave studies*. In ”/Earthquake source asymmetry, structural media and rotation effects/” eds. Tisseyre et al., Springer Verlag (2006).
- Schreiber K.U., J.-P. R. Wells, G.E. Stedman; *Noise Processes in Large Ring Lasers*. Journal General Relativity and Gravity (GRG), Vol 40, No 5, 935, DOI 10.1007/s10714-007-0584-2, (2008)
- Stedman, G. E. (1997); Ring laser tests of fundamental physics and geophysics. Rep. Progr. Phys. 60:615–688, (1997)
- Suryanto, W., H. Igel, A. Cochard, B. Schuberth, D. Vollmer, F. Scherbaum, K.U. Schreiber, A. Velikoseltsev; *First comparison of array-derived rotational ground motions with direct ring laser measurements*. Bull. Seism. Soc. Am., 2059:2071 – 96 (2007)
- Takeo M., H. M. Ito; *What can be learned from rotational motions excited by earthquakes?* Geophys. J. Int., 129:319 – 329, (1997)
- Takeo M.; *Ground rotational motions recorded in near-source region of earthquakes*. Geophys. Res. Lett., 25, 789–792, (1998)
- Wassermann, J., S. Lehndorfer, H. Igel, K.U. Schreiber, ; *Performance Test of a Commercial Rotational Motions Sensor*. Bull. Seism. Soc. Amer., submitted, (2008)
- Wilkinson, J. R. (1987), Prog. Quant. Electr. Vol. 11, 1–103 *Ring Lasers*, (1987)

## 7. TABLE

TABLE I: List of earthquakes discussed in this thesis.

Date	Time	Lat.	Lon.	Mag.	Region	Dist.	S/N	S/N	Phase vel.	Peak Corr.
	(UTC)	[°]	[°]			[°]	(Acc.)	(Rot.)	[ $ms^{-1}$ ]	Coeff.
2006/04/20	23:25:20	167.08	60.95	7.6	Kamchatka	54.81	528	94	5197	0.95
2006/05/24	04:20:28	-115.27	32.44	5.4	Mexico	1.53	4313	590	4648	0.92
2007/05/20	09:40:43	32.97	-115.92	3.6	California	0.78	561	34	8670	0.96
2007/05/24	06:11:39	34.20	-117.38	3.9	California	0.97	14352	97	14512	0.98

## 8. FIGURE LEGENDS

**Figure 1:** Construction diagram of the GEOsensor ring laser.

**Figure 2:** The complete ring laser mechanics mounted on a rigid concrete slab in an underground laboratory (left). The lever system with one of the mirrors inside the vacuum enclosure is used to align the laser cavity under UHV conditions (right).

**Figure 3:** Time-series of the instantaneous measured rate of rotation of the GEOsensor taken at the Piñon Flat observatory.

**Figure 4:** Example of two small local tremors measured in Piñon Flat. The observed rotation rates are up to 150 nrad/s.

**Figure 5:** Sudden longitudinal mode changes cause disruptions in the interferogram. Normally these effects occur quite rapidly. Ground motion between such mode changes is retrievable.

**Figure 6:** Sudden longitudinal mode changes, within the laser, can result in the simultaneous presence of two modes with different longitudinal indices. For as long as this state of operation persists there is no detectable audio beat frequency.

**Figure 7:** 2006.04.20 Kamchatka M 7.6 event: superposition of the vertical component of rotation rate (dashed) in rad/s and transverse acceleration (solid line, scaled to match in amplitude) recorded by the GEOsensor plus the corresponding maximum cross-correlation coefficients in a 20 s sliding time window for a backazimuth of  $324.5^\circ$ .

**Figure 8:** 2006.05.24 Mexico M 5.4 event: superposition of the vertical component of rotation rate (dashed) in rad/s and transverse acceleration (solid line, scaled to match in amplitude) recorded by the GEOsensor plus the corresponding maximum cross-correlation coefficients in a 20 s sliding time window for a backazimuth of  $139.2^\circ$ .

**Figure 9:** 2007.05.20 California M 3.6 event: superposition of the vertical component of rotation rate (dashed) in rad/s and transverse acceleration (solid line, scaled to match in amplitude) recorded by the GEOSensor plus the corresponding maximum cross-correlation coefficients in a 2 s sliding time window for a backazimuth of  $144.7^\circ$ .

**Figure 10:** 2007.05.24 California M 3.9 event: superposition of the vertical component of rotation rate (dashed) in rad/s and transverse acceleration (solid line, scaled to match in amplitude) recorded by the GEOSensor plus the corresponding maximum cross-correlation coefficients in a 1 s sliding time window for a backazimuth of  $307.7^\circ$ .

Figure 1

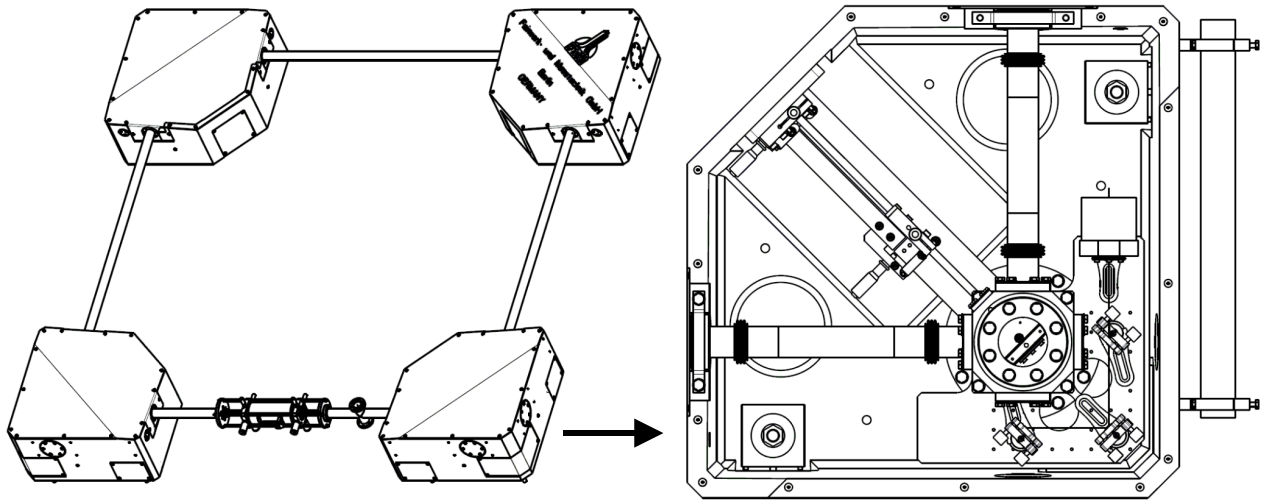


FIG. 1:

Figure 2

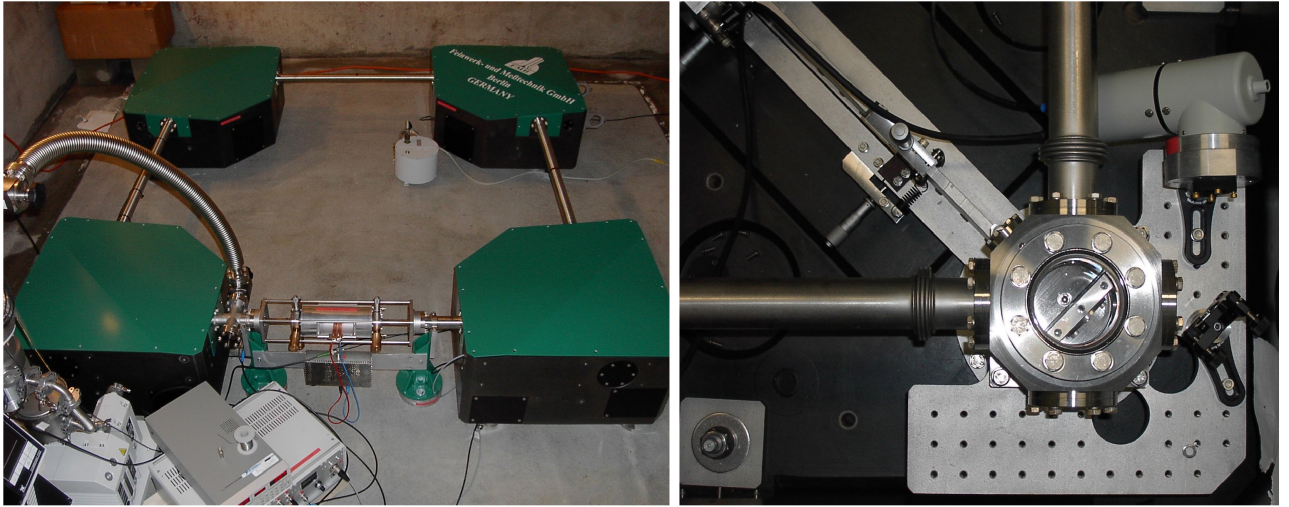


FIG. 2:

Figure 3

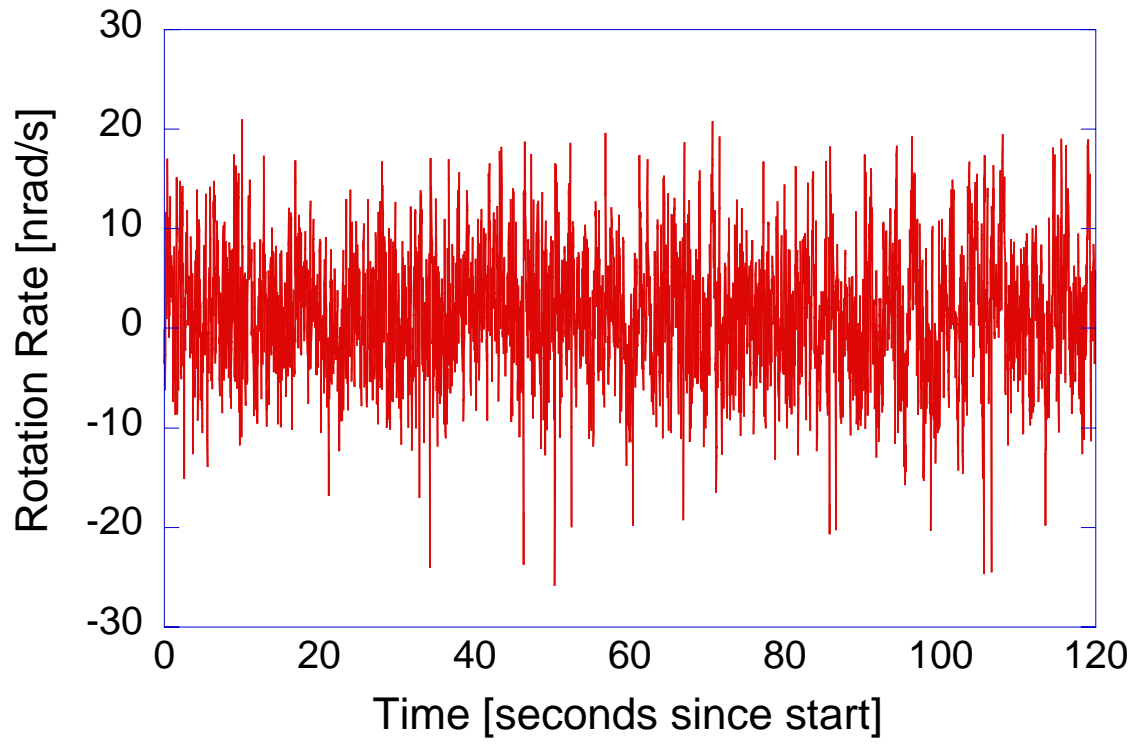


FIG. 3:

Figure 4

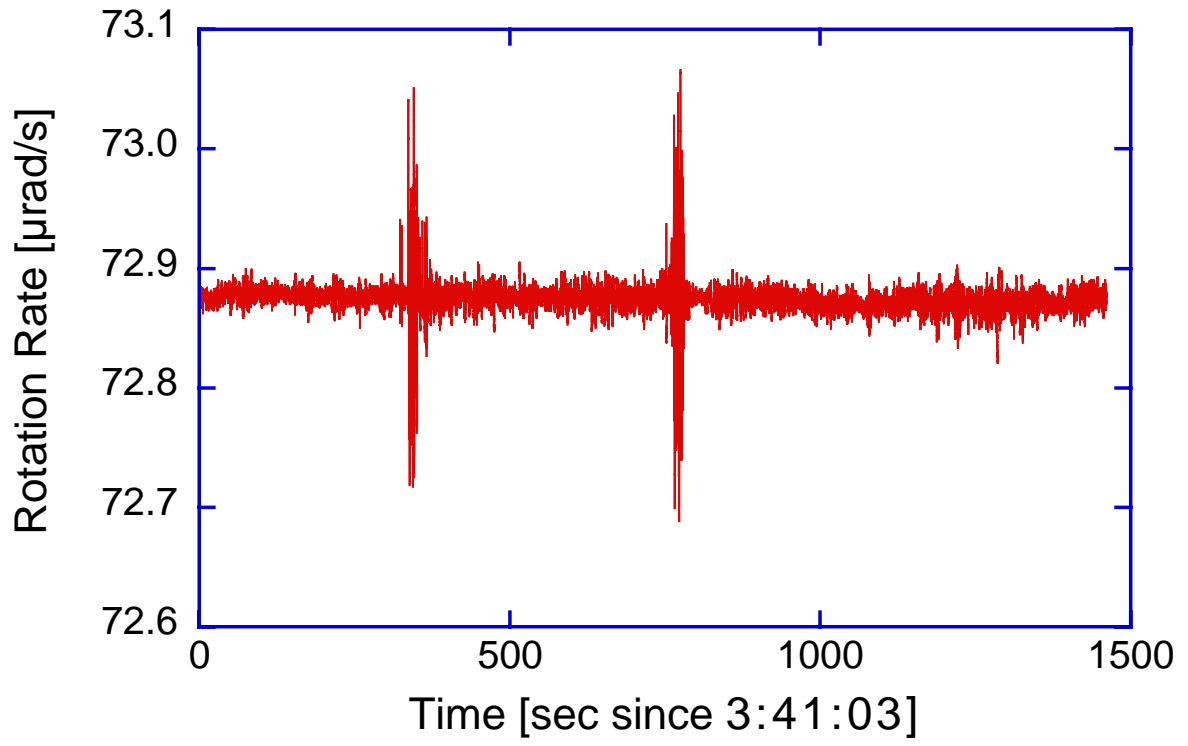


FIG. 4:

Figure 5

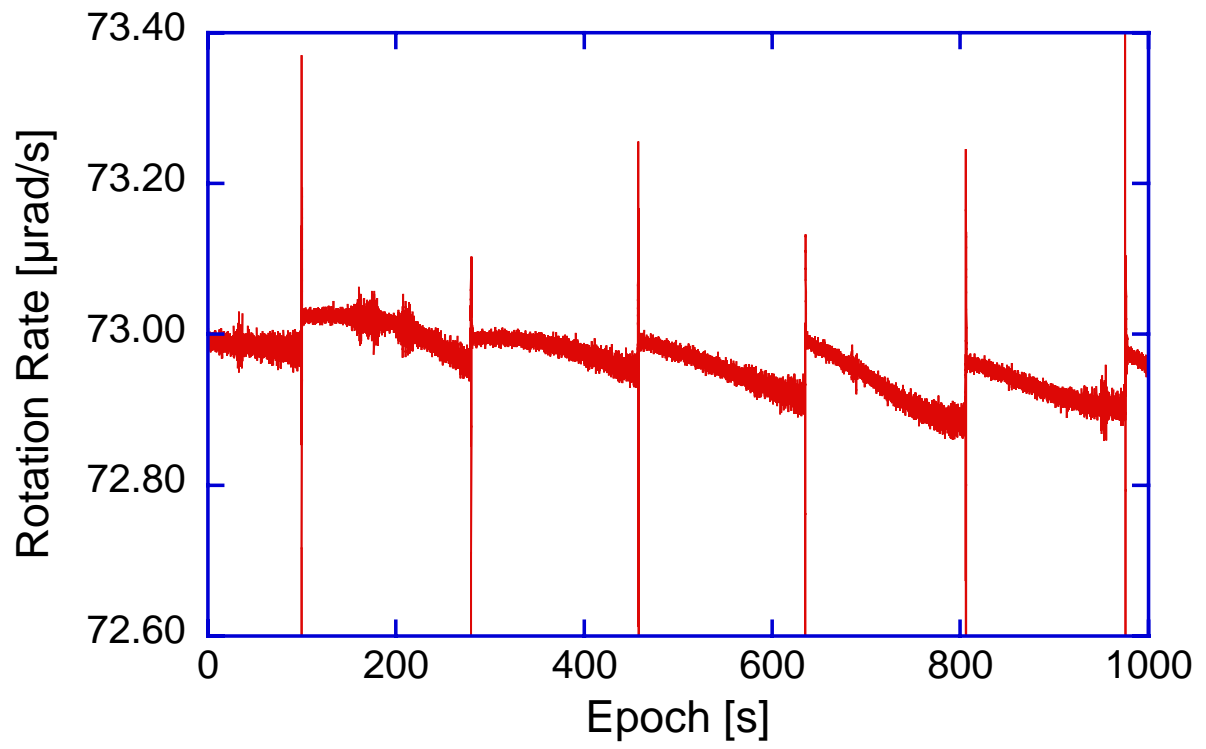


FIG. 5:

Figure 6

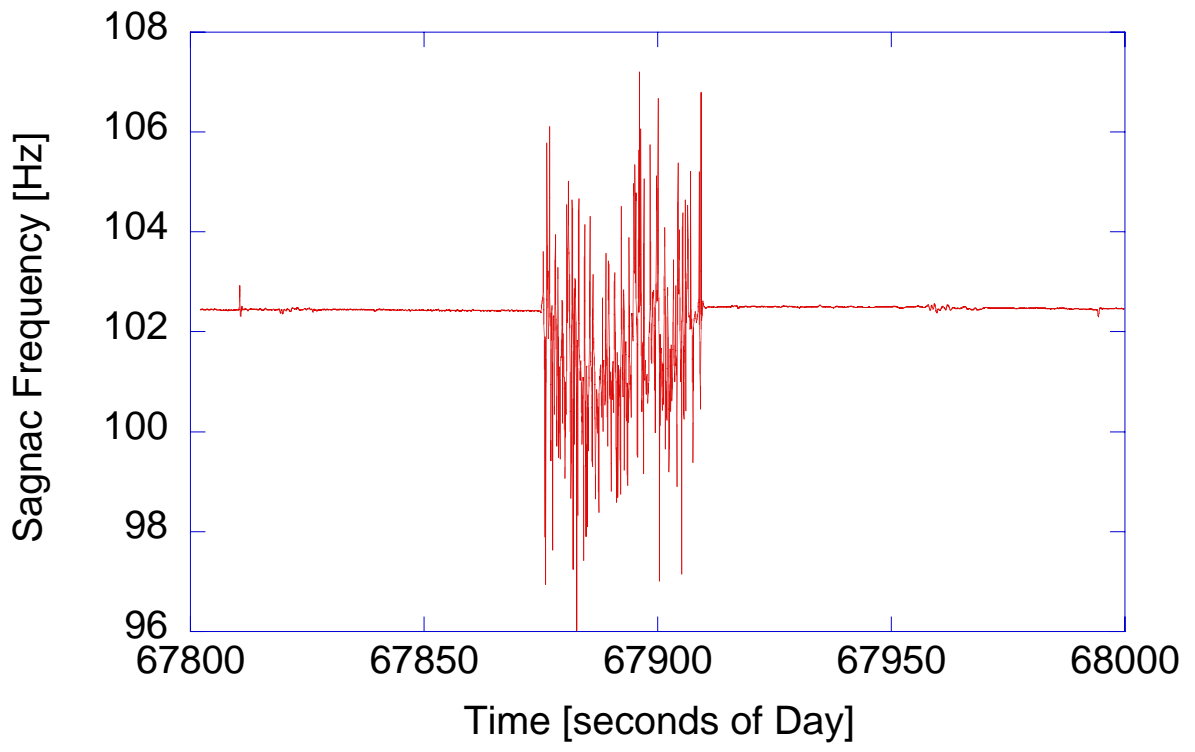


FIG. 6:

Figure 7

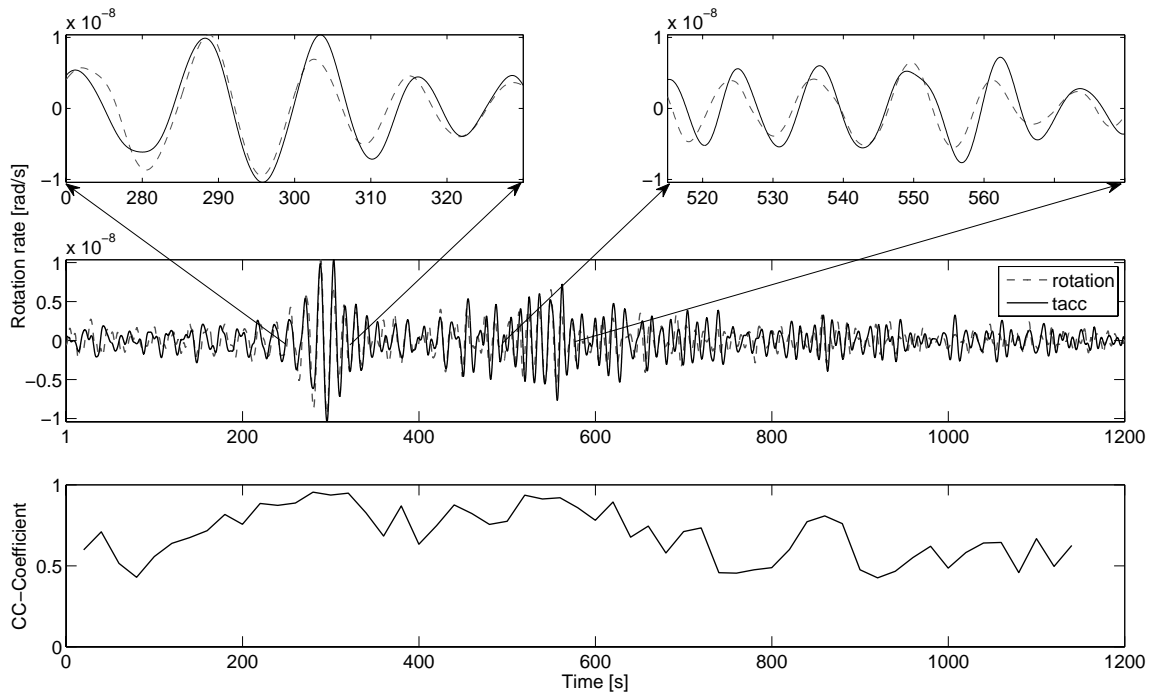


FIG. 7:

Figure 8

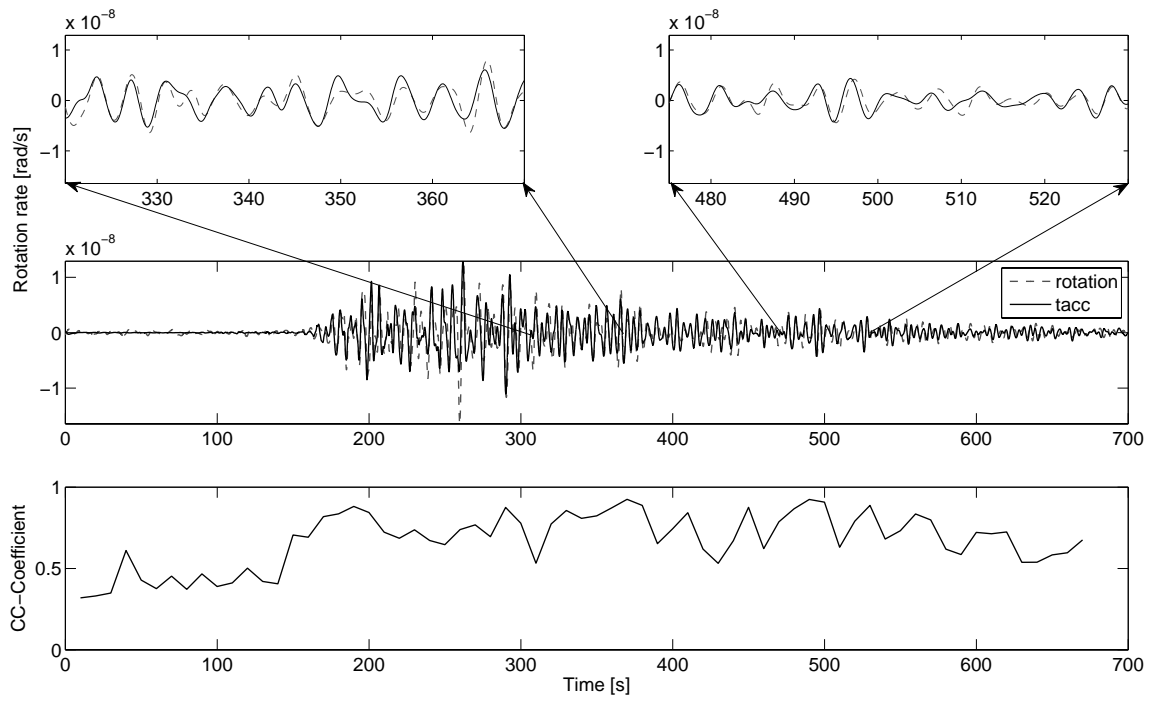


FIG. 8:

Figure 9

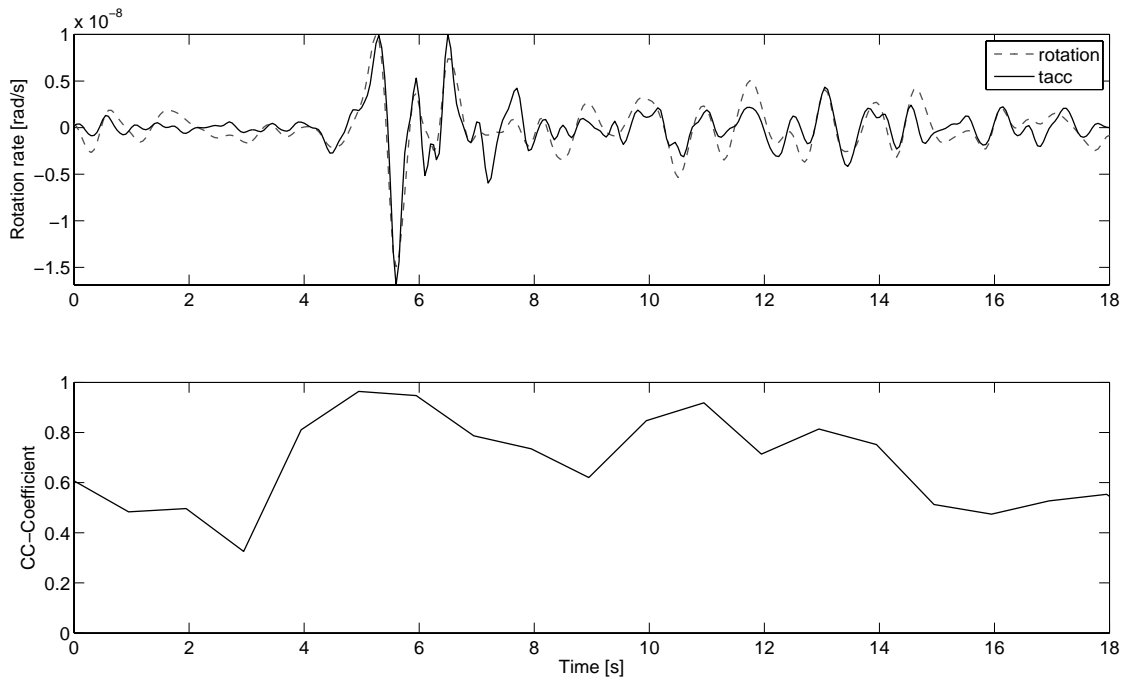


FIG. 9:

Figure 10

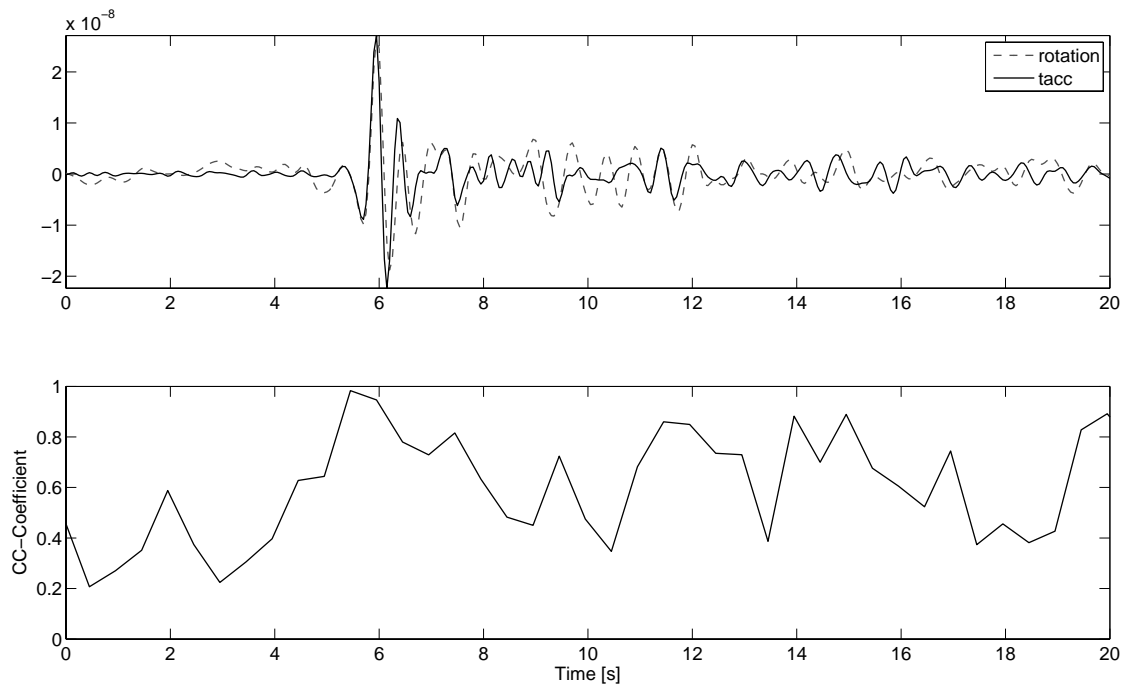


FIG. 10: